JOURNAL OF BACTERIOLOGY, Nov. 2009, p. 7027–7038 Vol. 191, No. 22
0021-9193/09/$12.00 doi:10.1128/JB.00948-09

A Novel Regulatory Protein Involved in Motility of *Vibrio cholerae*▽

Manuel Moisi,[1] Christian Jenul,[1] Susan M. Butler,[2]† Aaron New,[2]§ Sarah Tutz,[1] Joachim Reidl,[1] Karl E. Klose,[3] Andrew Camilli,[2] and Stefan Schild[1]*

Institut fuer Molekulare Biowissenschaften, Karl-Franzens-Universitaet Graz, Humboldtstrasse 50, 8010 Graz, Austria[1]; Howard Hughes Medical Institute and the Department of Molecular Biology and Microbiology, Tufts University School of Medicine, Boston, Massachusetts 02111[2]; and South Texas Center for Emerging Infectious Diseases, Department of Biology, University of Texas at San Antonio, San Antonio, Texas 78249[3]

Received 20 July 2009/Accepted 3 September 2009

The facultative pathogen *Vibrio cholerae* is the causative agent of the human intestinal disease cholera. Both motility and chemotaxis of *V. cholerae* have been shown to contribute to the virulence and spread of cholera. The flagellar gene operons are organized into a hierarchy composed of four classes (I to IV) based on their temporal expression patterns. Some regulatory elements involved in flagellar gene expression have been elucidated, but regulation is complex and flagellar biogenesis in *V. cholerae* is not completely understood. In this study, we determined that the virulence defect of a *V. cholerae cheW1* deletion mutant was due to polar effects on the downstream open reading frame VC2058 (*flrD*). Expression of *flrD* in *trans* restored the virulence defect of the *cheW1* deletion mutant, and deletion of *flrD* resulted in a *V. cholerae* strain attenuated for virulence, as determined by using the infant mouse intestinal colonization model. The *flrD* mutant strain exhibited decreased transcription of class III and IV flagellar genes and reduced motility. Transcription of the *flrD* promoter, which lies within the coding sequence of *cheW1*, is independent of the flagellar transcriptional activators FlrA and RpoN, which activate class II genes, indicating that *flrD* does not fit into any of the four flagellar gene classes. Genetic epistasis studies revealed that the two-component system FlrBC, which is required for class III and IV flagellar gene transcription, acts downstream of *flrD*. We hypothesize that the inner membrane protein FlrD interacts with the cytoplasmic FlrBC complex to activate class III and IV gene transcription.

The causative agent of cholera is the gram-negative facultative human pathogen *Vibrio cholerae* (34). *V. cholerae* is highly motile via its single sheathed polar flagellum. The sodium driven rotary motor complex of the *Vibrio* flagellum can turn at rates as high as 1,700 revolutions/s and produces speeds up to 60 μm/s in liquid media (3, 4).

Not surprisingly, the synthesis of an important cellular structure like the flagellum is tightly regulated. Flagellar gene transcription is organized in a transcriptional hierarchy, which has been categorized into four gene classes (50) (see Fig. 7). The only class I gene identified so far encodes the σ^{54} (RpoN)-dependent activator FlrA, which together with the RpoN-holoenzyme of RNA polymerase (RNAP) activates the expression of class II genes. These genes comprise mainly those for structural components, like the MS (membrane/supramembrane) ring and export apparatus components, but also include chemotaxis genes and genes encoding regulatory factors, including FlhG, FlhF, the two-component system FlrBC, and σ^{28} (FliA). FlhG is a negative regulator of class I gene transcription, while FlhF stimulates class III gene transcription, most likely by interaction with the FlrBC system (15). The response regulator FlrC, along with the RpoN holoenzyme, directly activates transcription of class III genes, which encode components of the basal body and hook, as well as the main flagellin, FlaA. FlrC must be phosphorylated by the sensor histidine kinase FlrB to activate flagellar gene transcription, although the specific stimulating signals remain unknown (14). Unlike most other sensor histidine kinases, FlrB is a cytosolic soluble protein (14). The FliA holoenzyme activates the expression of class IV genes, which encode additional flagellins FlaBCDE, the motor complex, and the anti-sigma factor FlgM. FlgM prevents the association of FliA with RNAP (13); after complete assembly of the basal-body–hook structure, FlgM is secreted through the sheathed flagellum, which facilitates FliA association with RNAP and class IV transcription (13).

The presence of the flagellum and flagellum-mediated motility are crucial factors in several steps of the *V. cholerae* life cycle, which for the pathogenic strains is marked by transitions between the aquatic ecosystem and the human gastrointestinal tract. Several studies indicate a close association and interaction between *V. cholerae* and chitinous surfaces (e.g., zooplankton such as copepods) in the aquatic environment (12, 28, 48, 54). In this environment, *V. cholerae* utilizes chitin as a carbon and nitrogen source and induces natural competence (42, 43). *V. cholerae* also forms biofilms on chitinous surfaces, which is likely to be an important survival and persistence mechanism within the aquatic environment between epidemic outbreaks (52, 55). Flagellar motility is crucial for early steps during biofilm development, as it accelerates the attachment to abiotic surfaces and mediates spread along these surfaces (64). In later steps of biofilm formation, the flagellar motor complex appears

* Corresponding author. Mailing address: Institut für Molekulare Biowissenschaften, Karl-Franzens-Universitaet Graz, Humboldtstrasse 50, 8010 Graz, Austria. Phone: 43 (0)316 380-1970. Fax: 43 (0)316 380-9019. E-mail: stefan.schild@uni-graz.at.

† Present address: Department of Microbiology, New York University School of Medicine, 550 First Avenue, New York, NY 10016.

§ Present address: Department of Molecular and Microbial Systems, Katholieke Universiteit Leuven, B-3001 Leuven (Heverlee), Belgium.

▽ Published ahead of print on 18 September 2009.

to act as a mechanosensor, signaling the interaction with an abiotic surface and stimulating exopolysaccharide expression (36).

V. cholerae transits from the aquatic reservoir into the human host by oral ingestion of contaminated food or water. After passage through the stomach, the bacteria reach the small intestine, which is the primary site of colonization. Nonmotile mutants of the O1 El Tor biotype, which is currently the dominant clinical isolate, colonize 10 to 25 times less efficiently than wild-type (WT) strains (37, 38, 47). It has been proposed that flagellar motility supports the initial contact with the intestinal epithelial surface and is necessary for the penetration through mucus (9, 18, 19). Recently, it was demonstrated that breakage of the flagellum during mucin penetration allows secretion of the anti-σ^{28} factor FlgM through the damaged flagellum (13, 38). This decrease of intracellular FlgM releases the alternative sigma factor FliA, which results in activation of FliA-dependent genes and inhibits the HapR-mediated repression of virulence genes. Thus, the flagellar biosynthesis pathway and virulence gene regulation are linked, and this interaction is important for full expression of virulence genes (38). Two recent studies which focused on the late stage of infection indicated that *V. cholerae* has evolved genetic programs for the transition from the human host into the aquatic environment (49, 60). Detachment and escape from the mucosal surface after successful colonization are controlled by the stationary-phase sigma factor RpoS, which induces flagellar motility genes and activates the mucinase HapA via HapR (49). Interestingly, *V. cholerae* organisms shed by cholera patients are transiently more infectious than in vitro-cultured bacteria (44). Despite their being highly motile, the hyperinfectious phenotype of stool bacteria is marked by a repression of chemotaxis genes, which enhances survival of the bacteria in a new host (8–10). Consistent with this observation, smoothly swimming counterclockwise (CCW)-biased nonchemotactic mutants of *V. cholerae* have a significantly lower infectious dose and outcompete the WT strain in the infant mouse colonization model (8, 10). Mathematical modeling of human epidemiological data supports the hyperinfectivity phenomenon as one explanation for the rapid and explosive outbreaks caused by *V. cholerae* (24).

In the present study, we characterized the role of VC2058 in virulence, motility, and regulation of flagellar synthesis. Due to the functional properties of VC2058 (see below), we have renamed it the flagellar regulatory protein D (*flrD*). Deletion of *flrD* results in a strain that is less motile and attenuated for virulence in the infant mouse colonization model, demonstrating a role for this gene in both the motility and virulence of *V. cholerae*. We further show that *flrD* is expressed from a promoter located within the coding sequence of *cheW1* that is independent of FlrA and RpoN, regulators of class II transcription. Although *flrD* is expressed independently of the established flagellar hierarchy, it is a positive regulator of class III and IV flagellar genes.

MATERIALS AND METHODS

Strain construction and growth conditions. Bacterial strains and plasmids used in this study are listed in Table 1, oligonucleotides are listed in Table 2. Unless noted otherwise, strains were grown with aeration in Luria-Bertani (LB) broth at 37°C. *V. cholerae* AC51, a spontaneous streptomycin-resistant mutant of *V. cholerae* O1 El Tor clinical isolate C6709 was used as a WT strain in all experiments (56). For genetic manipulations, *Escherichia coli* strains DH5α, DH5αλpir, and SM10λpir were used (23, 35, 45). Antibiotics and other supplements were used in the following final concentrations: streptomycin (Sm), 100 μg/ml; ampicillin (Ap), 50 μg/ml in combination with other antibiotics or 100 μg/ml; kanamycin, 50 μg/ml; arabinose, 0.02%; and isopropyl-β-D-thiogalactopyranoside, 0.1 mM.

DNA manipulations and construction of suicide plasmids and mutant strains. Chromosomal DNA was prepared using a DNeasy tissue kit, whereas PCR products and digested plasmid DNA were purified using Qiaquick gel extraction and Qiaquick PCR purification kits (Qiagen). PCRs for sequencing and subcloning were carried out using the Easy-A high-fidelity PCR cloning enzyme (Stratagene), *Pfu* polymerase (Stratagene), or Phusion high-fidelity polymerase (New England Biolabs). For all other reactions, *Taq* DNA polymerase (New England Biolabs) was used. Automated DNA sequencing was performed either with an automated ABI 3130XL DNA sequencer or with an ABI Prism 310 automated sequencer.

Deletion mutations were generated by SOE (splicing by overlap extension) PCR (27). All deletions are in frame, and the sequences deleted are listed in Table 1. The resulting PCR products were initially cloned into the pCR-Script Amp SK vector (Stratagene), followed by subcloning into the pCVD442-*lac* plasmid using SphI and SacI restriction sites that had been incorporated into the primers used for PCR amplification. The pCVD442-*lac* derivatives were transformed into *E. coli* Sm10λpir and subsequently moved into *V. cholerae* via conjugation.

To construct plasmid pGPphoAflrD, first the promoterless *phoA* gene was PCR amplified from Sm10λpir with the oligonucleotide pair phoA-XbaI-5′ and phoA-XbaI-3′. The resulting PCR fragment containing the full coding sequence of *phoA*, including the Shine-Dalgarno site, was then digested with XbaI and ligated into pGP704 that had been digested similarly, resulting in pGPphoA. Next, an *flrD* fragment was PCR amplified using oligonucleotide primers VC2058-SacI and VC2058-KpnI, and the resulting fragment, containing the translational stop codon of *flrD*, was digested with SacI and KpnI and ligated into pGPphoA that had been digested similarly, resulting in pGPphoAFlrD. Thus, the *flrD* fragment was now located upstream of *phoA* and separated from it by at least one stop codon. The plasmid was transformed into SM10λpir to allow conjugation into *V. cholerae*. Insertion of pGPphoAflrD into the *flrD* locus on the *V. cholerae* chromosome by homologous recombination results in a transcriptional fusion of *phoA* to the *flrD* transcript.

To construct plasmid pGPflaA, an internal fragment of *flaA* was PCR amplified with the oligonucleotide pair flaA-SacI and flaA-XbaI, digested with SacI and XbaI, and ligated into pGP704 that had been digested similarly.

Conjugation was achieved by cross-streaking the donor *E. coli* strain carrying the plasmid with the recipient *V. cholerae* strain on an LB plate and then incubating at 37°C for ~6 h. Plasmid cointegrants were then selected by isolation of colonies on LB Sm^r/Ap^r medium. For generation of chromosomal deletions with pCVD442 derivatives, isolated colonies were then grown in LB broth in the absence of antibiotics, followed by growth on LB plates with sucrose to obtain Ap^s colonies. Correct insertions or chromosomal deletions were confirmed by PCR (data not shown).

Construction of expression plasmids. All expression plasmids using pMMB67EH, pFLAG-MAC, or pBAD18-Kan were constructed in a similar manner. PCR fragments of the respective gene were generated using the oligonucleotide pairs designated in the format *x*-*y*-5′ and *x*-*y*-3′, in which *x* stands for the gene and *y* for the restriction site/enzyme used (Table 2). PCR fragments were digested with the respective restriction enzymes and ligated into similarly digested pMMB67EH, pFLAG-MAC, or pBAD18-Kan. The M114I mutation in FlrC was generated by SOE PCR, using pBKflrC as a template and oligonucleotide pairs flrC-M114I-up and flrC-SacI-5′ as well as flrC-M114I-down and flrC-XbaI-3′. The two PCR products were used as the template in the second PCR with flrC-SacI-5′ and flrC-XbaI-3′, and the resulting fragment was digested with SacI and XbaI and ligated into similarly digested pBAD18-Kan.

Construction of promoter-*lacZ* fusions. The plasmid series pRS551′cheW′-I through pRS551′cheW′-V was constructed by introducing different upstream fragments of *flrD* into pRS551. PCR fragments were generated using one of the oligonucleotides cheW-I through cheW-V as a forward primer paired with cheW-BamHI as the reverse primer. Thus, one end of each PCR product was located 28 bp downstream of the *flrD* start codon. PCR products were digested with EcoRI and BamHI and ligated into pRS551 that had been similarly digested.

Motility assays. Swarm plates composed of 1% tryptone, 0.5% NaCl, and 0.3% agar were used to assess motility of *V. cholerae* strains. Strains were first grown overnight at 37°C, then a single colony was inoculated by toothpick into the swarm plate, and the plate was incubated for 24 h at room temperature.

TABLE 1. Strains and plasmids used in this study

Strain or plasmid	Description	Reference
E. coli		
DH5α	F$^-$ Δ(*lacZYA-argF*)*U169 recA1 endA1 hsdR17 supE44 thi-1 gyrA96 relA1*	23, 35
DH5αλpir	F$^-$ Δ(*lacZYA-argF*)*U169 recA1 endA1 hsdR17 supE44 thi-1 gyrA96 relA1* λ::*pir*	23, 35
SM10λpir	*thi recA thr leu tonA lacY supE RP4-2-Tc*::*Mu* λ::*pir*	45
V. cholerae		
AC51	El Tor C6709; Sm^r	56
AC66	Insertion of *res-tet-res* in *lacZ* of AC51; Sm^r Tc^r	11
Δ*flrD* mutant	Deletion of *flrD* (+2 to + 167) in AC66; Sm^r Tc^r	This work
Δ*cheW1* mutant	Deletion of *cheW1* (+2 to + 159) in AC66; Sm^r Tc^r	This work
Δ*cheY3* mutant	Deletion of Δ*cheY3* in AC66, Sm^r Tc^r	10
cheW1(*G69D*) mutant	AC66 *cheW1*(*G69D*); Sm^r Tc^r	10
Δ*flrC* mutant	Deletion of *flrC* in AC51; Sm^r	This work
Δ*flrA* mutant	Deletion of *flrA* (+2 to + 488) in AC51; Sm^r	This work
rpoN mutant	Insertion of a pGP704 derivative in *rpoN* of AC51; Sm^r Ap^r	This work
Plasmids		
pCVD442	*ori6K mobRP4 sacB* Ap^r	17
pCVD442-lac	pCVD442::*lacZ*	17
pGP704	*ori6K mobRP4* Ap^r	45
pKEK84	pCVD442::Δ*flrC*	32
pΔ*flrA*	pCVD442-lac::Δ*flrA*	This study
pΔ*flrD*	pCVD442-lac::Δ*flrD*	This study
pΔ*cheW1*	pCVD442-lac::Δ*cheW1*	This study
pGPflaA	pGP704::*flaA*	This study
pGPrpoN	pGP704::*rpoN*	33
pGPphoA	pGP704 with promoterless *phoA* of SM10λpir	This work
pGPphoAflrD	pGPphoA with *′flrD′* fragment of AC51	This work
pRS	pRS551, transcriptional *lacZ* fusion vector Ap^r, Km^r	61
pKEK72	*flrB* promoter-*lacZ* fusion in pRS551	33
pKEK73	*flrA* promoter-*lacZ* fusion in pRS551	33
pKEK79	*flaB* promoter-*lacZ* fusion in pRS551	32
pKEK80	*flaA* promoter-*lacZ* fusion in pRS551	32
pRS'cheW'-I	Upstream fragment (497 bp) of *flrD* and 28 bp of *flrD* in pRS551	This work
pRS'cheW'-II	Upstream fragment (458 bp) of *flrD* and 28 bp of *flrD* in pRS551	This work
pRS'cheW'-III	Upstream fragment (325 bp) of *flrD* and 28 bp of *flrD* in pRS551	This work
pRS'cheW'-IV	Upstream fragment (204 bp) of *flrD* and 28 bp of *flrD* in pRS551	This work
pRS'cheW'-V	Upstream fragment (125 bp) of *flrD* and 28 bp of *flrD* in pRS551	This work
pMMB	pMMB67EH, IncQ broad-host-range low-copy-number cloning vector	46
pflrD	*flrD* of AC51 in pMMB67EH Ap^r	This study
pFLAG-MAC	Expression vector of Met-N-terminal FLAG fusion proteins Ap^r	Sigma-Aldrich
pFLAG-flrD	*flrD* of AC51 in pFLAG-MAC Ap^r	This work
pFLAG-flrD-31	*flrD* missing AA 1 to 31 of AC51 in pFLAG-MAC Ap^r	This work
pBK	pBAD18-Kan, araBADp cloning vector, Km^r	22
pBKflrC	*flrC* of AC51 in pBAD18-Kan; Km^r	This work
pBKflrCM114I	*flrC* with point mutation M114I of AC51 in pBAD18-Kan; Km^r	This work

Competition assays. Competition assays for intestinal colonization in infant mice (in vivo) and for growth in LB broth (in vitro) were performed with a mixture of mutant (Lac$^-$) and isogenic WT (LacZ$^+$) strains as previously described (11). The competitive index (CI) represents the ratio of mutant to WT CFU recovered at 24 h, normalized to the input ratio. For competition assays involving mutants complemented with an expression plasmid, the corresponding WT strain carried the empty plasmid vector. The pMMB vector and its derivatives are well maintained in *V. cholerae*, and no significant loss of the plasmids was observed during in vivo passage (46).

RNA purification, qRT-PCR, and mapping of transcription start sites with the 5′ RACE method. RNA purification and quantitative reverse transcriptase PCR (qRT-PCR) were performed as described previously (60). Briefly, RNA was isolated from at least five independent mid-exponential-phase LB broth cultures (optical density at 600 nm [OD_{600}], 0.5 to 0.55). DNA was removed using a DNA-free kit (Ambion), and cDNA was synthesized from 1 μg RNA using a SuperScript first-strand synthesis system for qPCR (Invitrogen). Controls lacking reverse transcriptase were included. qRT-PCR experiments were performed with SYBR brilliant green qPCR Master Mix, utilizing a Stratagene Mv3005P real-time cycler and MxPro qPCR software (Stratagene). Each reaction mixture contained 300 nM primers, 100 ng template, and ROX reference dye. Each independent sample was tested in triplicate. The sequences of the primers used in these studies are in Table 2, labeled in the format *x*-F and *x*-R, in which *x* stands for the respective gene and F and R indicate forward and reverse primers. All primer pairs amplified the target gene with efficiencies of 97% or more (data not shown).

For each sample, the mean cycle threshold of the test transcript was normalized to that of *rpoB* and to one randomly selected reference sample of the WT. Values of >1 and <1 indicate that the transcript is present in higher and lower numbers, respectively, in the mutant than in the WT.

The +1 transcriptional start site of the *flrD* gene was identified using a 5′ RACE (rapid amplification of cDNA ends) system (Invitrogen) according to the instruction manual. Briefly, RNA was isolated and treated with DNase as described above. Total RNA (1 to 5 μg) was used to synthesize cDNA from the 5′ end of the *flrD* mRNA with the gene-specific primer GSP1-flrD. The reaction was performed with the SuperScriptII RT at 42°C for 50 min. A homopolymeric C tail was added to the cDNA with the terminal deoxynucleotidyl transferase. The RACE products were synthesized using the abridged anchor primer AAP and the gene-specific primer GSP2-flrD followed by a second PCR to reamplify the primary product using the universal amplification primer UAP and a nested

TABLE 2. Oligonucleotides used in this study

Primer	Sequence (5′ to 3′)[a]
VC2058-1-SacI	CGAGCTCGGCAAAATGGGTAATGGCTGAG
VC2058-2	TAAGCCATACTACATTCTTCATCGGTCAGG
VC2058-3	CGATGAAGAATGTAGTATGGCTTATTTCCT
VC2058-4-SphI	ACATGCATGCCGGTTCATCCAAAATCCACAG
cheW-1-SphI	ACATGCATGCTTGCTCAGTCAGTTGGAATCG
cheW-2	GAAAATTAAAACATTGGGTGAACAAGTTCCT
cheW-3	CATTGGGTGAACAAGTTCCTGACCGATGAAG
cheW-4-SacI	CGAGCTCGTATGGCGGTGAGATTTTTAAC
flrA-1-SphI	ACATGCATGCTATTTGGCCGAGCACCCTG
flrA-2	ATGGTTTCCCTACATAGGTGAGATTATTTGCCT
flrA-3	ATCTCACCTATGTAGGGAAACCATAGTCAATAT
flrA-4-SacI	CGAGCTCCTTTCGACTTCTTGACCG
VC2058-SacI-5′	CGAGCTCGGGCAAACTACTGATTCTGGTG
VC2058-SphI-3′	ACATGCATGCCTTCAAAAACTCATTCAG
VC2058-HindIII-5′	AAATTCGAAGGACGAAATGGCTCATATGTA
VC2058/31-HindIII-5′	AAAAAGCTTCTGGCATTGTGGCGTCTTAAA
VC2058-EcoRI-3′	AAAGAATTCCTATGATTTGGCTTTGTTGGCTCGAA
flaA-SacI	TTTGAGCTCTCATCAGGTAATCGCATTAA
flaA-XbaI	TTTTCTAGAACCGATTTGGAACGAAGCTT
flrC-SacI-5′	AAAGAGCTCAGAGACTGGAGAGTGAAGA
flrC-XbaI-3′	TTTTCTAGATTTGTATGCCATGCCCTCAACC
flrC-M114I-up	GTAACGGCTGAC**AAT**ATTCAGCAGCACTTCTGGTG[b]
flrC-M114I-down	CACCAGAAGTGCTGCTGAATA**TT**GTCAGCCGTTAC[b]
cheW-I	AAAGAATTCGGAAACGACTCAGAGAGGGA
cheW-II	AAAGAATTCAATGAAGTGAAAGTCAGAAAA
cheW-III	TTTGAATTCTGTACCGGGAGCGCCTGA
cheW-IV	TTTGAATTCATCATTGTGATTGAGTCAGAA
cheW-V	TTAGAATTCAGAAATTGACTCAACCCCAAGT
cheW-BamHI	ATAGGATCCATTACATATGAGCCATTT
phoA-XbaI-5′	TTTTCTAGATTTTTAATGTATTTGTACATGGAGAA
phoA-XbaI-3′	TTTTCTAGAGTGATCTGCCATTAAGTCTGGTT
VC2058-SacI	AAAGAGCTCGGACAAAAAGTCAGTGAGCAA
VC2058-KpnI	AAAGGTACCCTATGATTTGGCTTTGTTGGCTCGA
rpoB-F[c]	CTGTCTCAAGCCGGTTACAA
rpoB-R[c]	TTTCTACCAGTGCAGAGATGC
VC2058-F	GTACACTCGTGCCAGTAAGATG
VC2058-R	GAACTTCGGGATGACTTTCCAG
AAP	GGCCACGCGTCGACTAGTAGTACGGGIIGGGIIGGGIIG
UAP	CUACUACUACUAGGCCACGCGTCGACTAGTAC
GSP1-flrD	CCATTTCGTCCCAT
GSP2-flrD	CATCACGATTGCTCACACCTTGG
GSP3-flrD	CTTTCATCGGTGCCCACACTTG
fliA-F	GAGAACTCAATCGCGATCCAAC
fliA-R	CCGAGATCCTCTATCCCAACAA
flhA-F	GGTCGTGGTCAAAGTTCTACAG
flhA-R	CTTGACTCTTACTCGCGTATTCCG
flrA-F	TAGCTCGGTTGAAGAGCAAGAG
flrA-R	GGCGCATCTATATCAGGGACAAAC
flrB-F	CAGGTATTGGATGTGATGCC
flrB-R	CGAGTGGTACATCCAGTAAACG
flaA-F	GGTCGTAAGCTACTCAATGGTTCG
flaA-R	CGGAAATCATCAGCACGTACACTG
flaG-F	CAACGTCTTAACGAGGAGCAAC
flaG-R	TCGTAGATAGTAACCACCTCGC
flaB-F	GAAGCGGTATCTATTCTGGATGGGC
flaB-R	CCAAGTTACTGATCGCATGACC
motY-F	CCGTAATGTCAGCCTAGTCTCT
motY-R	CAGTTCACTGAGTAACGACCAC

[a] Restriction sites are underlined.
[b] Bold indicates codons changed to obtain desired amino acid mutations.
[c] Oligonucleotides for *rpoB* are according to reference 53.

gene-specific primer GSP3-flrD. The RACE products were directly sequenced to identify transcription start sites.

Cellular fractionation. The fractionation protocol was adapted from the work of Bose and Taylor (6). A late-exponential-phase LB broth culture (500 ml; $OD_{600} \sim 1$) was harvested by centrifugation, washed once with LB broth, and resuspended in 10 mM Tris-HCl (pH 8) with Complete protease inhibitor mix (Roche). Cell extracts were obtained by passing the resuspended cell solution through a French pressure cell at 1,000 lb/in^2, followed by a low-speed centrifugation at 4,500 $\times$ *g* at 4°C for 20 min to remove intact cells. The whole-cell lysate was then centrifuged at 10,000 $\times$ *g* at 4°C for 30 min for further purification, before membranes were separated from the supernatant by centrifugation at 75,000 $\times$ *g* at 4°C for 30 min. In order to solubilize the inner membrane

proteins, the membrane pellet was resuspended in 10 mM Tris-HCl (pH 8), 100 mM NaCl, and 2.5% Sarkosyl, incubated with gentle rocking for 30 min, and then centrifuged at 75,000 × *g* at 4°C for 1 h. The supernatant was retained as the inner membrane fraction, and the pellet containing the outer membrane was resuspended in 1 ml of 10 mM Tris-Cl (pH 8.0). Protein estimation was carried out using a Lowry protein assay kit (Pierce) with bovine serum albumin as the standard. Whole-cell lysates for the detection of FlaA were prepared as follows: 500 μl of a log-phase culture (OD_{600} = 0.5) was harvested by centrifugation, and the cell pellet was resuspended and boiled in 100 μl protein sample buffer. Protein concentration was estimated using sodium dodecyl sulfate-polyacrylamide gel electrophoresis followed by Coomassie staining.

Immunoblot analysis. Equal amounts of proteins from whole-cell lysates, as well as corresponding cell equivalents of cellular fractions, were separated by sodium dodecyl sulfate-polyacrylamide gel electrophoresis and transferred onto a nitrocellulose membrane (Invitrogen). Immunoblot analysis was performed as described previously (59). The membrane was blocked by incubation with 10% skim milk in TBS (10 mM Tris-Cl [pH 7.5], 150 mM NaCl) for 2 h at room temperature. The membrane was washed twice in TBS-TT (20 mM Tris-Cl [pH 7.5], 500 mM NaCl, 0.05% Tween 20, 0.2% Triton X-100) and once in TBS for 10 min each. Primary antibodies used were mouse polyclonal FlaA antibodies (this study), rabbit polyclonal OmpT antibodies (51), or mouse monoclonal anti-FLAG M2 antibody (Sigma). The appropriate primary antibody diluted 1:1,000 in 10% skim milk in TBS was added to the transfer membrane and incubated with gentle rocking at 4°C overnight, followed by washing as described above. The membrane was then incubated for 1 h in TBS 10% skim milk containing the appropriate secondary antibody (horseradish peroxidase-conjugated sheep anti-mouse or donkey anti-rabbit immunoglobulin [GE Healthcare UK Limited]). The membrane was then washed four times in TBS-TT for 10 min each. Chemiluminescence was detected by using the ECL Plus Western blotting detection system (GE Healthcare UK Limited) and exposure to X-ray film (Kodak).

Alkaline phosphatase (PhoA) and β-galactosidase (LacZ) assays. To determine the enzymatic activities for the transcriptional *phoA* and *lacZ* fusions, alkaline phosphatase and β-galactosidase assays were performed as described previously (39, 57, 58). The activities are expressed in Miller units, calculated as $(A_{405} \times 1{,}000)/(A_{600} \times \text{ml} \times \text{min})$.

Statistical analysis. Data were analyzed using the Mann-Whitney U test, by a Kruskal-Wallis test followed by post-hoc Dunn's multiple comparisons, or by a Wilcoxon signed rank test against a hypothetical value of 1. Differences were considered significant for *P* values of <0.05.

RESULTS

FlrD enhances *V. cholerae* intestinal colonization of infant mice. As reported previously, nonchemotactic CCW-biased mutants of *V. cholerae* (e.g., the *cheY3* or *cheR* mutant) have a competitive advantage over the WT during infection of infant mice (8, 10). Consistent with these findings, a nonchemotactic CCW-biased mutant with a point mutation in *cheW1* [*cheW1*(*G69D*)] outcompetes WT in vivo (10). In *E. coli*, this point mutation disrupts the interaction of CheW with CheA and the Tar complex, resulting in a smooth swimming nonchemotactic phenotype (7). Additionally, it has been demonstrated that the *cheW1*(*G69D*) strain colonizes the intestine, similar to another nonchemotactic CCW-biased mutant, the Δ*cheY3* mutant (10). These results with the *cheW1*(*G69D*) mutant are consistent with the phenotype expected of a nonchemotactic CCW-biased mutant. Interestingly, *V. cholerae* strains with in-frame deletions of *cheW1* did not exhibit the same phenotype as the strain containing the *cheW1* point mutation. For example, a Δ*cheW1* mutant exhibits a fivefold colonization defect in vivo in competition against a Δ*cheY3* strain (Fig. 1). This defect in colonization is not due to a growth defect of the Δ*cheW1* strain, since the Δ*cheW1* and Δ*cheY3* strains compete equally for in vitro growth. Additionally, chemotaxis and colonization defects of a Δ*cheW1* mutant could not be restored by expression of *cheW1* in *trans* (10) (data not shown). This argues

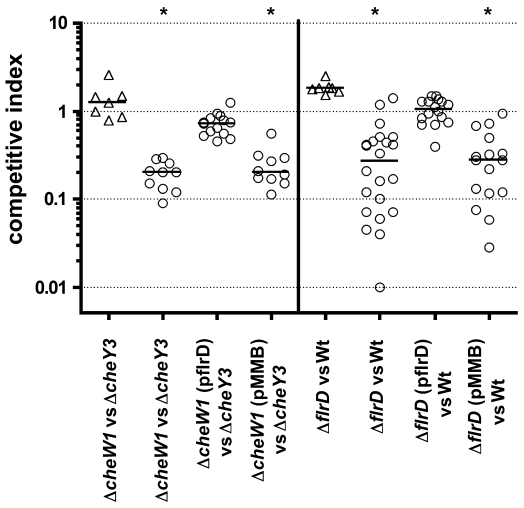

FIG. 1. Colonization phenotypes of *V. cholerae* WT and mutant strains. Results are shown as the CI for competition in LB broth (triangles) and in vivo using the infant mouse model (circles). Strains used in the competition assays are indicated on the *x* axis. Each shape represents the CI from a single assay. The horizontal bars indicate the median of each data set. The asterisks indicate significantly different medians of the in vivo competitions compared to the respective in vitro competitions ($P < 0.05$, using a Mann-Whitney U test).

for a polar effect of the Δ*cheW1* deletion on downstream genes, since these phenotypes are absent in the *cheW1*(*G69D*) point mutant strain. We hypothesized that the deletion of *cheW1* reduces expression of the downstream located *flrD*, which in turn leads to reduced fitness in vivo.

In support of this hypothesis, the colonization defect of Δ*cheW1* strain was significantly rescued by the expression of *flrD* in *trans* on a low-copy-number plasmid but not by the plasmid vector alone (Fig. 1). To investigate the function of FlrD in more detail, a *V. cholerae* strain with an in-frame deletion in *flrD* (Δ*flrD*) was constructed. The Δ*flrD* strain exhibited a fourfold colonization defect compared to the WT strain in the infant mouse intestine (Fig. 1). This defect could be complemented back to WT levels of colonization by expression of *flrD* in *trans* in the Δ*flrD* strain, while colonization was not enhanced in the Δ*flrD* strain carrying the plasmid vector alone. It should be noted that the Δ*flrD* strain had a small but significant (twofold) fitness advantage over the WT in an in vitro competition assay ($P < 0.05$, using a Wilcoxon signed rank test).

The promoter of *flrD* is located in *cheW1*. The polar effect of a deletion of *cheW1* on *flrD* expression suggests there is an active promoter within the *cheW1* coding region which is required for transcription of *flrD*. To demonstrate the existence of an active promoter element within *cheW1*, we constructed chromosomal transcriptional fusions of a promoterless *phoA* reporter gene to *flrD* in the WT, Δ*cheW1*, and *cheW1*(*G69D*) strains. The resulting PhoA activity reflects the expression levels of *flrD* in the respective strains (Fig. 2A). The WT and the *cheW1*(*G69D*) strains exhibited comparable levels of PhoA activity, which indicates similar *flrD* expression levels in these strains. In contrast, the Δ*cheW1* strain showed significantly decreased levels of PhoA activity in comparison to the WT. These results argue for the existence of an active promoter

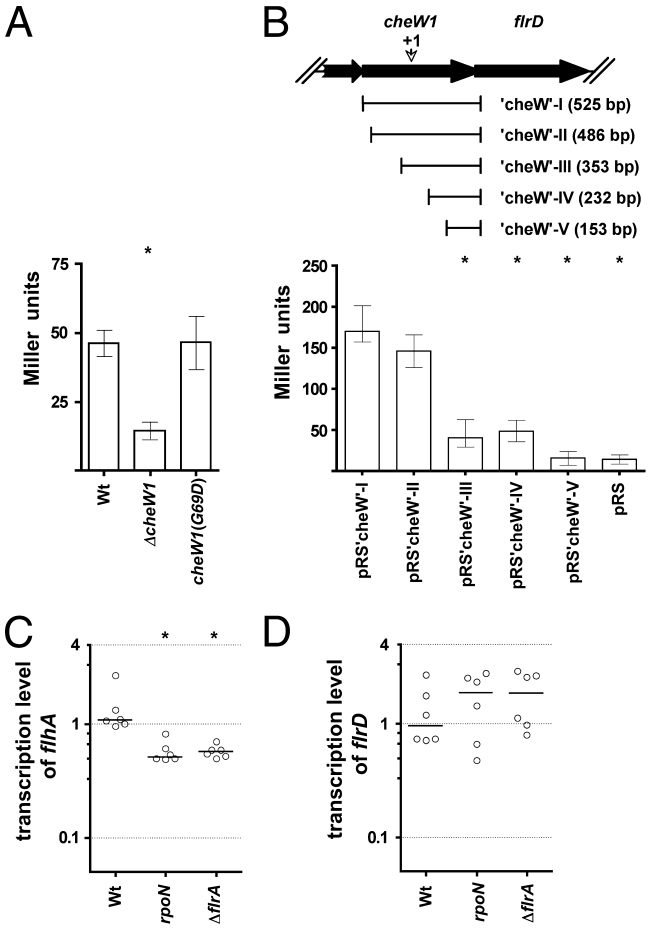

FIG. 2. Characterization of the *flrD* promoter. (A) Alkaline phosphatase activities (in Miller units) of the WT and of *cheW1* mutants with a chromosomal *flrD-phoA* transcriptional fusion. The asterisk indicates a median significantly different from the WT data set ($P < 0.05$, Mann-Whitney U test). (B, bottom) β-Galactosidase activities (in Miller units) of AC66 carrying pRS or derivatives with different-sized fragments of the *flrD* upstream region (′cheW′-I to -V). (B, top) Location and length of each fragment with respect to the *cheW1* locus. All fragments ended 28 bp after the *flrD* start codon but started at different position within *cheW1*. The position of the +1 transcription start site identified by 5′ RACE is indicated. The asterisks indicate a significant decrease in activity compared to the pRS′cheW′-I data set ($P < 0.05$, Kruskal-Wallis test and post-hoc Dunn's multiple comparisons). Results in panels A and B are the medians from at least five independent experiments. The error bars indicate the interquartile range of each data set. (C and D) Ratio of transcripts of *flrD* (C) and *flhA* (D) to *rpoB* (control) for the WT as well as an *rpoN* and a *flrA* mutant. Each data set was normalized to one randomly selected reference sample. Each circle represents the qRT-PCR result from an independent culture. The horizontal bar indicates the median of each data set. The asterisks indicate a significant decrease of the *flhA* transcript levels in the *rpoN* and Δ*flrA* mutants compared to the WT ($P < 0.05$, Mann-Whitney U test).

within *cheW1* that drives expression of *flrD* and that is absent in the deletion mutant.

To characterize the *flrD* promoter in more detail, different-sized fragments of the *flrD* upstream region were analyzed for their promoter activity. We constructed plasmids containing the upstream region fragments (′cheW′-I to -V) fused to *lacZ* and then measured transcription levels of *lacZ* in the WT strain carrying these plasmids (Fig. 2B). All fragments end 28 bp downstream of the *flrD* start codon, but they start at different positions in *cheW1*. The largest fragment (′cheW′-I; 525 bp) comprises the entire coding region of *cheW1*. The two largest fragments, 486 and 525 bp, fused to *lacZ* expressed the highest β-galactosidase activity, while the smaller fragments, 353, 232, and 153 bp, fused to *lacZ* showed significantly lower β-galactosidase activity. These results demonstrate the presence of an active promoter within *cheW1* that drives transcription of *flrD*. Additionally, 5′ RACE was carried out to determine the transcriptional start site of the *flrD* mRNA. The results place the +1 transcriptional start site 282 bp upstream of the *flrD* start codon. Additionally, a highly conserved putative −10 region with the sequence TATTAT was identified upstream of the +1 start site at the proper distance. Thus, the +1 start site was present in the fragments ′cheW′-I to -III. Since this transcriptional start site is located very close to the 5′ end of the ′cheW′-III fragment, it is not surprising that this fragment exhibited only low promoter activities. Additional upstream elements and the correct DNA topology might be important for full promoter activity, and these are obviously present in the two largest fragments, ′cheW′-I and -II. In summary, *flrD* should no longer be assigned to the upstream operon starting with *flhA*.

The promoter of *flrD* is RpoN (σ^{54}) and FlrA independent. The flagellar gene operon upstream of *flrD*, encompassing genes from *flhA* to *cheW1*, has previously been shown to be RpoN and FlrA dependent and has therefore been assigned to flagellar gene class II (50). We measured transcription levels of *flhA* by qRT-PCR, which confirmed that *flhA* transcripts were significantly reduced in *rpoN* and *flrA* mutants compared to the WT (Fig. 2C). In contrast, transcript levels of *flrD* were not significantly altered in *rpoN* or *flrA* mutants compared to the WT (Fig. 2D). This indicates that the promoter of *flrD* is RpoN and FlrA independent and that *flrD* does not belong to the class II flagellar genes. This is also further evidence that *flrD* is not part of the class II operon starting with *flhA* but rather has its own differentially regulated promoter.

FlrD is necessary for full expression of class III and IV flagellar genes. The proximity of *flrD* to other flagellar and chemotaxis genes prompted us to determine whether *flrD* is involved in motility and/or chemotaxis. We inoculated the strains into soft-agar plates, which are used to detect defects in motility and chemotaxis (Fig. 3A). The chemotactic motility of the WT strain produces a characteristic swarm as the bacteria swim away from the point of inoculum. In comparison to the WT, the Δ*flrD* strain produced a swarm with a much smaller diameter. This defect was complemented by expression of *flrD* in *trans* but not by the vector alone. To determine whether the reduced swarming ability of the Δ*flrD* strain in soft agar was due to motility or chemotaxis, we measured the expression of the major flagellin FlaA in the WT and Δ*flrD* strains by immunoblot analysis with an anti-FlaA antibody, using whole-cell lysates (Fig. 3B). FlaA (40.2 kDa) was detected in the whole-cell lysate of the WT strain but not in the whole-cell lysate of Δ*flrD*. Expression of FlaA was restored in the Δ*flrD* strain by expression of *flrD* in *trans* but not by the plasmid vector alone. These results demonstrate reduced expression of the class III flagellin FlaA in the Δ*flrD* strain, suggesting an effect of FlrD on the flagellar transcription hierarchy.

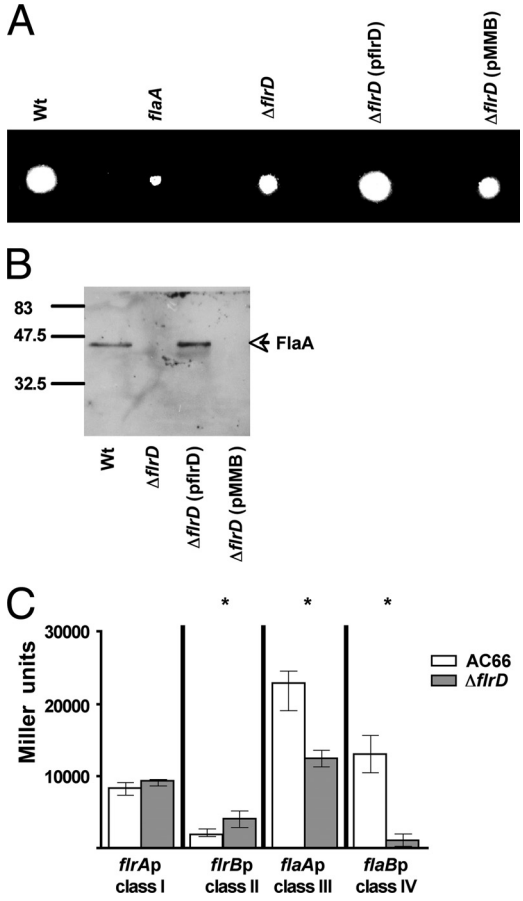

FIG. 3. Motility phenotypes and expression of flagellar genes in the WT and the Δ*flrD* mutant. (A) Analysis of motility by using swarm plates. (B) Detection of FlaA by immunoblot analysis using whole-cell lysates of the indicated strains. Equal amounts of protein were loaded. (C) β-Galactosidase activities (in Miller units) of AC66 and the Δ*flrD* strain carrying the flagellar gene promoter-*lacZ* fusion plasmid pKEK73 (*flrAp-lacZ*), pKEK72 (*flrBp-lacZ*), pKEK80 (*flaAp-lacZ*), or pKEK79 (*flaBp-lacZ*) with the respective promoter-*lacZ* fusion as well as the flagellar gene class indicated on the *x* axis. Values are the medians from at least five independent experiments. The error bars indicate the interquartile range of each data set. The asterisks indicate significantly different medians of activities of AC66 and the Δ*flrD* strain carrying the same plasmid ($P < 0.05$, Mann-Whitney U test).

To determine the effect of FlrD on the flagellar transcription hierarchy, we measured transcription of all four flagellar gene classes, using representative plasmids with flagellar gene promoter-*lacZ* transcriptional fusions in AC66 and Δ*flrD* (Fig. 3C). One representative promoter-*lacZ* fusion for each flagellar gene class was used. While *flrA* was transcribed at comparable levels in both strains, the Δ*flrD* strain showed a moderate increase in *flrB* transcription. This indicates that FlrD is not required for class I or class II gene transcription. In contrast, transcription of the class III gene *flaA* and the class IV gene *flaB* was significantly decreased in the Δ*flrD* strain compared to transcription of these genes in AC66, suggesting that FlrD enhances class III and IV flagellar gene transcription.

To confirm the effects of FlrD on the flagellar transcription hierarchy, we performed qRT-PCR of selected flagellar genes in the Δ*flrD* and WT strains (Fig. 4). Again, the two strains showed comparable transcription levels of the class I gene *flrA* (Fig. 4A), while class II *flrB* transcript levels were slightly, but not significantly, elevated in the Δ*flrD* strain (Fig. 4B). These results confirm that neither class I nor class II flagellar genes require FlrD for expression. In contrast, transcription levels of class III and IV genes were confirmed to be significantly decreased in the Δ*flrD* strain compared to the WT via qRT-PCR (Fig. 4C to F). Consistent with the results obtained with promoter-*lacZ* fusions, *flaA* (class III) and *flaB* (class IV) gene transcripts were significantly lower in the Δ*flrD* strain than the WT (Fig. 4C and E). We additionally measured transcripts for another class III gene, *flaG*, and another class IV gene, *motY* (Fig. 4D and F). These genes were also transcribed at significantly lower levels in the Δ*flrD* strain than the WT. These genes are located at different positions in the *V. cholerae* genome and consequently have their own promoters. Thus, FlrD is required for class III and IV gene expression in general, rather than being necessary for the activation of a specific flagellar gene operon.

In addition, qRT-PCR allowed us to study complementation of the decreased transcription of class III and IV genes. Transcription levels of *flaA*, *flaG*, *flaB*, and *motY* were restored in Δ*flrD* by expression of *flrD* in *trans*, while the empty vector alone had no effect. We also considered the possibility of a regulatory mechanism, whereby FlrD could act as an activator of the upstream located class II operon starting with *flhA*. However, transcription levels of two representative genes of the respective operon, *flhA* and *fliA*, were not significantly different in the Δ*flrD* strain (mean ± standard deviation, 1.5 ± 1.1 and 1.7 ± 1.3) and the WT (0.8 ± 0.3 and 1.2 ± 0.5).

Inner membrane localization of FlrD is necessary for function. Computational analysis of the protein sequence of FlrD revealed a putative transmembrane region predicted by several topology prediction programs (16, 25, 62, 63). Consistently, the topology models predict a transmembrane region from amino acids (aa) 18 to 33, with the N terminus located in the periplasm and the C terminus (aa 34 to 167) located in the cytoplasm. In order to investigate the membrane localization of FlrD, we constructed an expression vector that expressed FlrD with an N-terminal FLAG tag, which allowed detection of the protein by immunoblot analysis using an anti-FLAG antibody. The FLAG tag did not adversely affect the activity of FlrD, since expression of FLAG-FlrD in *trans* still rescued the motility defect of the Δ*flrD* strain, whereas the vector alone (pFLAG) was unable to rescue the motility defect of this strain (Fig. 5A). To determine whether membrane localization is important for FlrD activity, we also constructed an expression vector that expressed the truncated protein FLAG-FlrD-31, from which the N-terminal 31 aa, containing the putative transmembrane domain, had been removed. This truncated form of FlrD failed to rescue the motility defect of the Δ*flrD* strain (Fig. 5A), indicating that membrane localization is critical for FlrD function. The Δ*flrD* strain expressing either FLAG-FlrD or FLAG-FlrD-31 was used for fractionation experiments to determine the localization of the respective proteins (Fig. 5B). Immunoblot analysis of whole-cell lysates indicated that the two proteins were expressed at comparable levels. No degradation products were observed. Fractionation of inner and outer membrane compartments demonstrated that FLAG-FlrD is localized to the inner membrane, as predicted by the

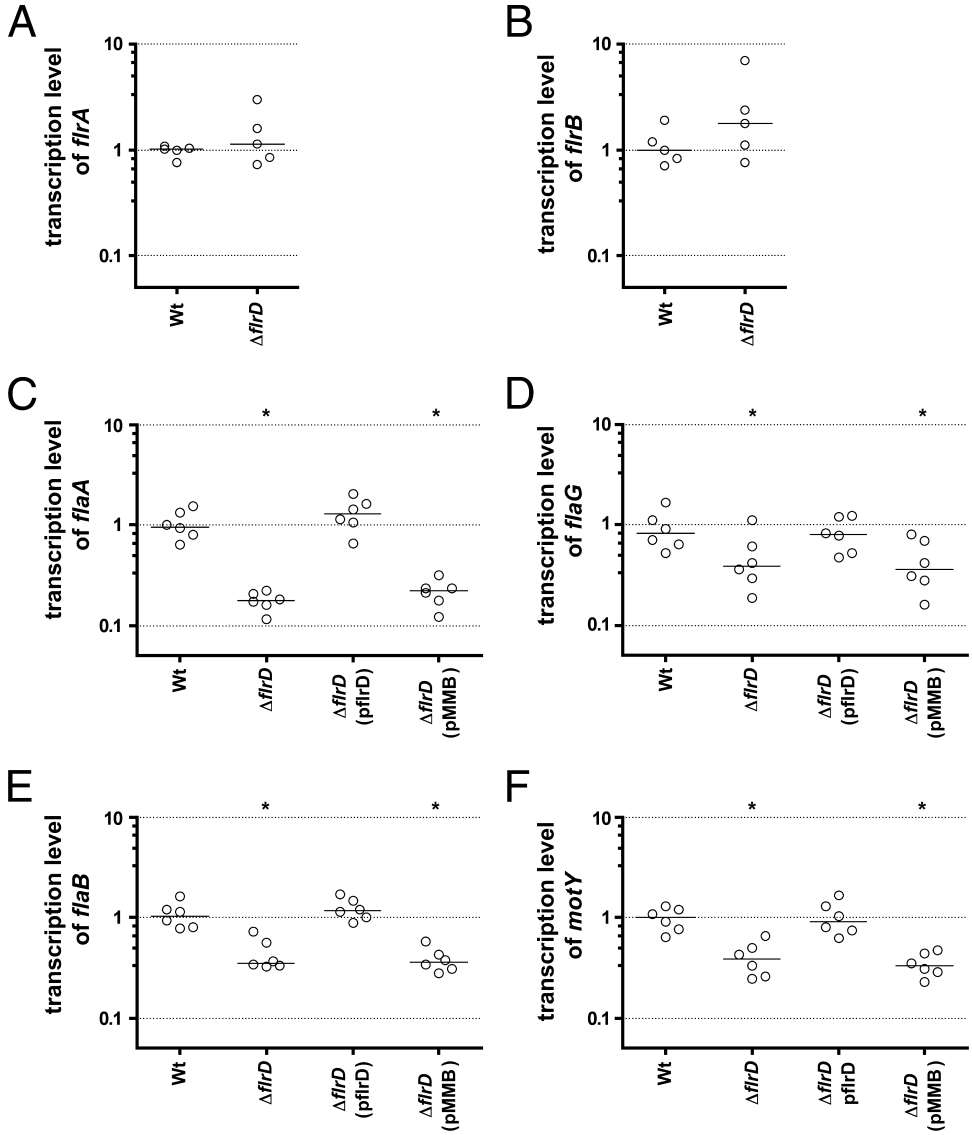

FIG. 4. qRT-PCR assessment of flagellar gene transcription in WT and Δ*flrD* strains. Values are ratios of transcripts of the flagellar genes indicated on the *y* axes to *rpoB* (control). Each data set was normalized to one randomly selected reference sample. Each circle represents an independent culture. The horizontal bar indicates the median of each data set. The asterisks indicate significantly different transcription levels of the respective genes compared to the WT data set ($P < 0.05$, Mann-Whitney U test).

topology prediction programs. In contrast, the truncated FLAG-FlrD-31 failed to localize to the inner membrane and remained in the cytoplasm (Fig. 5B). The outer membrane porin OmpT served as a loading control. OmpT should be detectable in all three fractions, since it is synthesized in the cytoplasm and from there transported to the outer membrane via the inner membrane and periplasm. Consequently, OmpT was present at high levels in the whole-cell lysate samples and outer membrane fractions but only at low levels in the inner membrane fractions.

The FlrBC two-component system acts epistatic over FlrD. The two-component regulatory system FlrBC directly activates transcription of class III flagellar genes, and class III gene expression is required for subsequent high-level transcription of class IV flagellar genes (33, 50). Our data indicate that FlrD, like FlrBC, is required for the transcription of class III and class IV flagellar genes. Due to the absence of a recognizable DNA-binding motif in FlrD, we speculated that FlrD might act upstream of FlrBC at the class II-class III checkpoint. FlrC requires phosphorylation by FlrB to activate transcription of class III genes (14), and thus, FlrD may influence the phosphorylation state of FlrC. We reasoned that high-level expression of FlrC or the FlrB-independent version FlrC-M114I in the Δ*flrD* strain should overcome the motility defect. The methionine-114-to-isoleucine (M114I) mutation allows constitutive FlrB-independent transcription of flagellar genes by FlrC but still requires phosphorylation of the aspartate (D54) by a noncognate kinase or acetyl-phosphate to activate flagellar gene transcription (14). FlrC and FlrC-M114I were expressed from a plasmid in the WT, Δ*flrC*, and Δ*flrD* strains. These

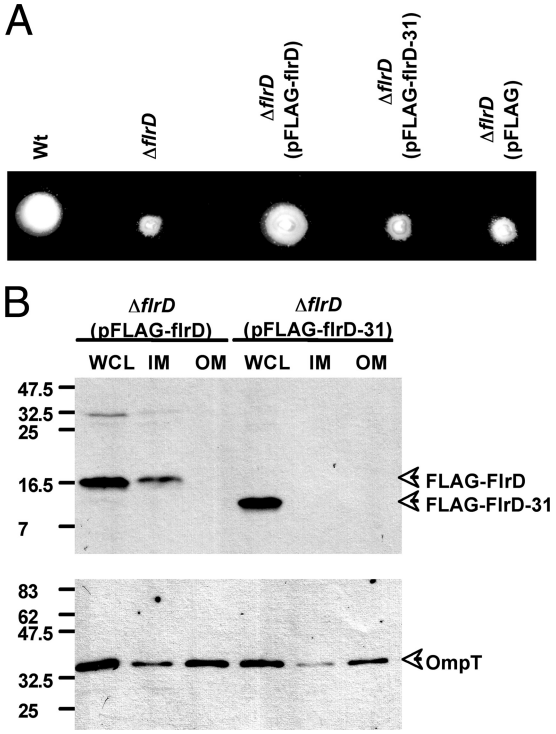

FIG. 5. Inner membrane localization of FlrD is important for activity. (A) Analysis of motility of the full-length FlrD and the N-terminal truncated version (missing the first 31 aa) by using swarm plates. (B) Immunoblot analysis of the whole-cell lysates (WCL) as well as inner (IM) and outer membrane (OM) fractions of the Δ*flrD* strain expressing either full-length FlrD (FLAG-FlrD) or a truncated form lacking 31 aa at the N terminus (pFLAG-FlrD-31).

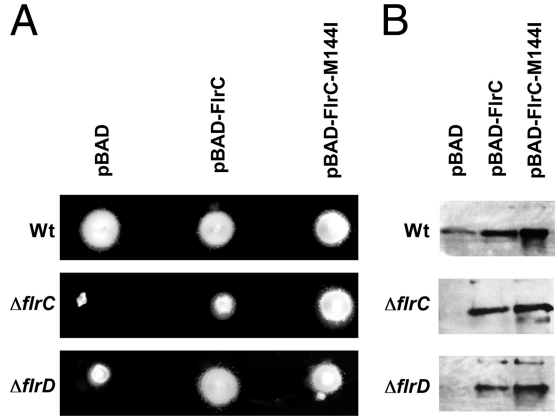

FIG. 6. Expression of FlrC rescues motility and FlaA expression in a *flrD* mutant. (A) Analysis of motility by using swarm plates. Wild-type and mutant strains carry pBAD or derivatives expressing either WT FlrC or the constitutively active FlrC-M114I version. (B) Detection of FlaA by immunoblot analysis using whole-cell lysates of the strains used for panel A. Equal amounts of protein were loaded.

strains were analyzed for their swarming ability (Fig. 6A). Furthermore, class III gene expression was evaluated by determining the level of FlaA expression in these strains by immunoblot analysis using an anti-FlaA antibody (Fig. 6B). The vector control had no effect on motility or on FlaA expression in any strain. As described above, the Δ*flrD* strain exhibited decreased motility compared to the WT, whereas the Δ*flrC* strain showed no swarming ability at all.

Overexpression of either FlrC or FlrC-M114I in the WT results in higher FlaA levels, demonstrating that levels of FlaA can increase even in the WT. However, the swarming ability of the WT expressing either type of FlrC in *trans* was slightly reduced, suggesting that overexpression of FlaA is disadvantageous for motility. Consistent with previous studies, the Δ*flrC* strain lacks FlaA expression, which can be restored by expression of either FlrC or FlrC-M114I in *trans* (14, 33). Although FlaA can be detected in whole-cell lysates of the Δ*flrC* strain expressing FlrC or FlrC-M114I, the motility defect is only partially complemented by FlrC but almost completely rescued by FlrC-M114I. Consistent with previous studies, expression of FlrC or FlrC-M114I in the Δ*flrC* strain rescued motility partially or almost completely (14, 33) (Fig. 6A). Expression of FlrC or FlrC-M114I in the Δ*flrD* strain also resulted in increased motility that was similar to WT levels, demonstrating that FlrBC is epistatic to FlrD. Measurement of FlaA levels in these strains by immunoblotting revealed that expression of FlrC or FlrC-M114I in *trans* in the Δ*flrC* and Δ*flrD* strains restores FlaA expression. The FlrB-independent form FlrC-M114I led to even higher levels of FlaA expression than the native FlrC (Fig. 6B). These results demonstrate that the motility defect of the Δ*flrD* strain can be overcome by overexpression of the activator of class III genes, FlrC, indicating that FlrD acts upstream of FlrBC with respect to the activation of class III and IV flagellar gene transcription.

DISCUSSION

To date, more than 40 gene products are known to participate in *V. cholerae* flagellar synthesis. The corresponding genes are organized into four classes and transcribed in a hierarchical fashion. In this study, we investigated the role of the uncharacterized gene *flrD*, which is located immediately downstream of *cheW1*, in a flagellar synthesis gene cluster. *flrD* was previously assigned to the flagellar class II gene operon, which starts with *flhA* (50). However, our results demonstrate that *flrD* is not part of this operon but rather is expressed from its own RpoN- and FlrA-independent promoter and thus appears to be transcribed independently of the four flagellar gene classes. Nevertheless, we also showed that FlrD positively regulates class III and IV flagellar gene transcription and contributes to intestinal colonization in the infant mouse model.

In addition to flagellar genes, the class II operon starting with *flhA* also encodes chemotaxis genes, including *cheY3*, *cheZ*, *cheA*, *cheB*, and *cheW1*. Interestingly, *V. cholerae* shed by cholera patients in planktonic form transiently represses chemotaxis genes while maintaining motility to increase infectivity (10, 44). These nonchemotactic bacteria, obtained from fresh stool samples from cholera patients, have a competitive advantage against in vitro-grown bacteria in infant mice and have a lower infectious dose. One hypothesis to explain the competitive advantage of *V. cholerae* found in stool samples suggests that nonchemotactic *V. cholerae* organisms avoid antimicrobial factors by their inefficient penetration of the intestinal crypts, whereas chemotactic bacteria follow the gradient of chemoat-

tractants into the intervillous spaces (9, 19, 20). In support of this hypothesis, nonchemotactic, CCW-biased mutants such as the *cheY3*, *cheR2*, and *cheW1*(*G69D*) strains are hyperinfectious and outcompete the WT strain about 30-fold during infection of the infant mouse intestine (8, 10).

Given the competitive advantage of nonchemotactic mutants for intestinal colonization, it was a surprise to find that a strain with a deletion of *cheW1*, which also results in a nonchemotactic CCW-biased phenotype, exhibits a colonization defect compared to other nonchemotactic mutants, e.g., the Δ*cheY3* mutant. Expression of *cheW1* in *trans* did not restore WT levels of motility and colonization to the Δ*cheW1* mutant, but it could restore normal chemotaxis and colonization to the *cheW1*(*G69D*) point mutant (10). Intrigued by this inconsistent result, we investigated the phenotype of the *cheW1* deletion in more detail. Using a transcriptional *phoA* fusion to the downstream-located *flrD*, we demonstrated that a deletion of *cheW1*, but not the G69D point mutation of *cheW1*, causes a decrease in transcription of *flrD*. Since a deletion of *flrD* by itself already results in a colonization defect in the infant mouse, the polar effect of Δ*cheW1* on *flrD* transcription is most likely responsible for the otherwise inexplicable reduced colonization capability of a *cheW1* deletion mutant. This is reinforced by the restored colonization fitness of Δ*cheW1* expressing *flrD* in *trans*. Thus, the current model concerning the hyperinfectious phenotype of nonchemotactic CCW-biased mutants is still valid.

The results also indicated that *flrD* is not part of the flagellar class II operon starting with *flhA*, and further analysis revealed that an active promoter for *flrD* lies within *cheW1*. According to the β-galactosidase activities and results from the 5′ RACE obtained in this study, the transcriptional start site of an active promoter element is located 282 bp upstream of the *flrD* start codon. Interestingly, the largest fragment analyzed for promoter activity contains a RpoN promoter consensus sequence with the conserved GG and GC elements in a 12-nucleotide distance (5). Such RpoN promoter consensus sequences are absent in all smaller fragments. Since the largest and second largest fragment showed quite similar promoter activities, the putative RpoN promoter does not significantly contribute to the transcription activation of *flrD*. Furthermore, we demonstrated by qRT-PCR analysis that *flrD* transcription was not altered in *rpoN* and *flrA* mutants. Hence, *flrD* is not a class II flagellar gene.

The data obtained using chromosomal *flrD-phoA* transcriptional fusions indicate that even in the Δ*cheW1*, mutant transcriptional activity can be observed. Thus, the promoter element in *cheW1* might be only one of several. However, according to our results the promoter element in *cheW1* is the most important one for *flrD* expression under the in vitro and in vivo conditions we investigated. Data obtained from previous studies also suggests a very complex regulation of the *flhA-cheW1* gene cluster. Besides RpoN and FlrA, RpoS was shown to be required for full expression of the gene cluster during stationary phase (49). This indicates that different promoters might activate the gene cluster in different growth phases. Hyperinfectious *V. cholerae* strains show high levels of expression of motility genes but reduced expression of genes required for bacterial chemotaxis (44). Thus, the flagellar and chemotaxis genes in the *flhA-cheW1* gene cluster have to be differentially regulated during the life cycle of *V. cholerae*.

The Δ*flrD* mutant exhibits decreased transcription of class III and IV flagellar genes, which causes reduced expression of the major flagellin FlaA and a motility defect on soft-agar plates. Analysis by electron microscopy revealed no obvious differences between the flagellum in the Δ*flrD* mutant and that in the WT (data not shown). However, as demonstrated in this study, the expression of class III and IV flagellar genes and motility is only reduced, not completely abolished, in Δ*flrD*. Thus, an effect of *flrD* on the morphology of the flagellum might not be readily identifiable by electron microscopy. Since flagellar motility contributes to virulence by facilitating attachment and penetration of the mucosal surface in the small intestine (18, 19), the reduced motility of the Δ*flrD* and Δ*cheW1* mutants is a likely explanation for the reduced colonization fitness in the infant mouse intestine. The involvement of *flrD*, which is not a class I or class II gene, in class III and IV gene expression places it into a novel gene class of the flagellar hierarchy, as shown in the proposed model (Fig. 7). Due to the lack of a conserved DNA-binding motif in FlrD, it is unlikely that FlrD directly activates transcription of class III and IV flagellar genes by binding to the promoter regions. Furthermore, our results indicate that the expression levels of important activators of class III and IV gene transcription, like the two-component system FlrBC, FlhF, and the alternative sigma factor FliA, are not altered in an *flrD* mutant.

The response regulator FlrC is the direct activator of class III genes and is also required for high-level transcription of class IV genes (50). Hence, it can be hypothesized that FlrD stimulates class III and IV gene transcription via the two-component system FlrBC. Our results demonstrate that transcription of *flrB* and consequently *flrC* is not dependent on FlrD. Thus, FlrD and FlrBC most likely interact on the protein level (Fig. 7). We showed that FlrD is a transmembrane protein, and localization to the inner membrane appears to be necessary for its function. The histidine kinase FlrB is a soluble cytosolic protein (14), and the specific conditions that activate FlrB are still unknown. However, completion of the MS ring-switch-export apparatus is the most likely signal for activation of FlrBC (15), but such a regulatory mechanism would probably require an interaction of the cytosolic FlrBC system with a membrane component. A Sequence Similarity DataBase search analysis allocated parts of FlrD to the PilN fimbrial assembly protein family (amino acids 10 to 148) and revealed a conserved HAMP domain (amino acids 20 to 86) (2, 29–31, 40). HAMP domains are usually found in integral membrane proteins that are part of signal transduction pathways. It is suggested that HAMP domains play a role in regulating the phosphorylation or methylation of receptors by transmitting conformational changes from the periplasm to the cytoplasm (2). This makes FlrD an ideal candidate for transferring signals, like the assembly of the MS ring-switch-export apparatus, to the FlrBC two-component system.

If this hypothesis is correct, activation of FlrC should overcome the motility defects in the Δ*flrD* strain. Accordingly, we analyzed whether FlrC is epistatic to FlrD by overexpression of the response regulator FlrC, as well as a FlrB-independent point mutant, FlrC-M114I (14). It is known that merely increasing the dosage of a response regulator can mimic the

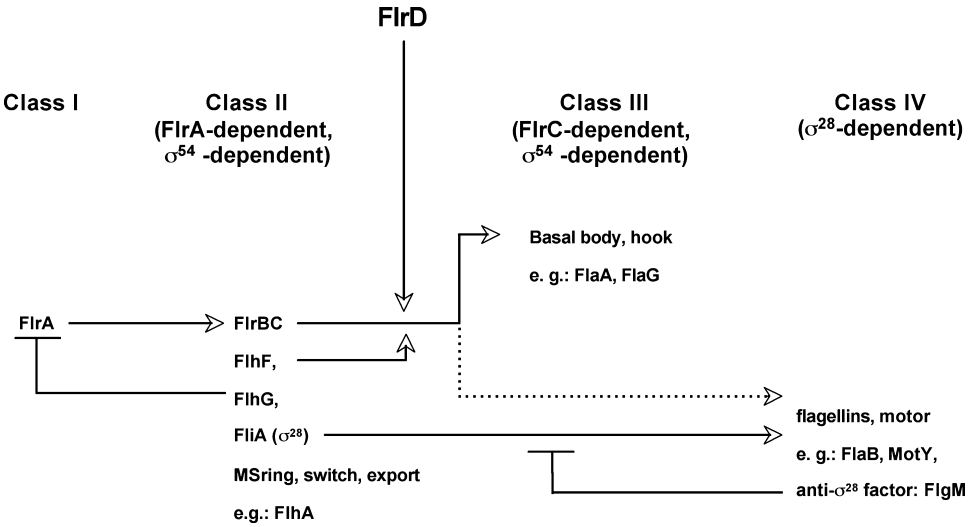

FIG. 7. Proposed function of FlrD in the regulation of the flagellar transcription hierarchy in *V. cholerae*. Shown is the model of flagellar gene regulation in *V. cholerae* according to Prouty et al. and Correa et al. (15, 50). The results present in this study indicate that FlrD acts as a positive regulator on class III and IV transcription. *flrD* cannot be classified as a class II gene, since its expression is independent of FlrA and RpoN. Thus, *flrD* represents a new flagellar gene class. The epistatic effect of FlrC over FlrD suggests an interaction of FlrD with the two-component system FlrBC. See Discussion for details.

effect of activation by phosphorylation (21, 26). Indeed, high-level expression of FlrC and especially FlrC-M114I rescued the motility defect of Δ*flrD* on soft-agar plates and restored expression of the flagellar class III protein FlaA. Our results suggest a potential interaction between the inner membrane protein FlrD and the two-component system FlrBC. It cannot be ruled out that FlrD does not directly interact with FlrBC, and instead another factor may be involved that interacts with FlrBC. A potential candidate for this would be FlhF, which has been previously characterized as an enhancer of class III and IV transcription (Fig. 7) (15).

Bioinformatic analysis using standard protein BLAST (BLASTP 2.2.21) revealed that FlrD is highly conserved within the order *Vibrionales* and conserved in other *Vibrio* spp., such as *Vibrio parahaemolyticus*, *Vibrio harveyi*, *Vibrio vulnificus*, and *Vibrio fischeri*, with identities of 50% or higher (1). Furthermore, FlrD homologues can also be found in other closely related *Gammaproteobacteria*, such as *Photobacterium* spp., *Aeromonas* spp., *Shewanella* spp., and *Pseudomonas* spp. (identities of 30% or higher), whereas FlrD seems not to be conserved in other bacteria, like *E. coli*. This is not surprising, since there are other genes like *flhF* and *flhG*, which are present in *Vibrio* spp. (and other bacteria), but are also not found in *E. coli* (41). Further studies are needed to elucidate the complex transcriptional regulation of *flrD* and the *flhA-cheW1* gene region as well as the protein-protein interactions involved in the class II-class III checkpoint in more detail.

ACKNOWLEDGMENTS

This work was supported by a grant from the Heinrich Jörg-Stiftung, Karl-Franzens Universität Graz, Austria, to S.S., by grant FWF-W901-B05 to J.R., and by NIH grant AI055058 to A.C. A.C. is a Howard Hughes Medical Institute Investigator.

REFERENCES

1. **Altschul, S. F., T. L. Madden, A. A. Schaffer, J. Zhang, Z. Zhang, W. Miller, and D. J. Lipman.** 1997. Gapped BLAST and PSI-BLAST: a new generation of protein database search programs. Nucleic Acid Res. **25:**3389–3402.
2. **Aravind, L., and C. P. Ponting.** 1999. The cytoplasmic helical linker domain of receptor histidine kinase and methyl-accepting proteins is common to many prokaryotic signalling proteins. FEMS Microbiol. Lett. **176:**111–116.
3. **Atsumi, T., Y. Maekawa, T. Yamada, I. Kawagishi, Y. Imae, and M. Homma.** 1996. Effect of viscosity on swimming by the lateral and polar flagella of *Vibrio alginolyticus*. J. Bacteriol. **178:**5024–5026.
4. **Atsumi, T., L. McCarter, and Y. Imae.** 1992. Polar and lateral flagellar motors of marine Vibrio are driven by different ion-motive forces. Nature **355:**182–184.
5. **Barrios, H., B. Valderrama, and E. Morett.** 1999. Compilation and analysis of σ^{54}-dependent promoter sequences. Nucleic Acids Res. **27:**4305–4313.
6. **Bose, N., and R. K. Taylor.** 2005. Identification of a TcpC-TcpQ outer membrane complex involved in the biogenesis of the toxin-coregulated pilus of *Vibrio cholerae*. J. Bacteriol. **187:**2225–2232.
7. **Boukhvalova, M. S., F. W. Dahlquist, and R. C. Stewart.** 2002. CheW binding interactions with CheA and Tar. Importance for chemotaxis signaling in *Escherichia coli*. J. Biol. Chem. **277:**22251–22259.
8. **Butler, S. M., and A. Camilli.** 2004. Both chemotaxis and net motility greatly influence the infectivity of *Vibrio cholerae*. Proc. Natl. Acad. Sci. USA **101:**5018–5023.
9. **Butler, S. M., and A. Camilli.** 2005. Going against the grain: chemotaxis and infection in *Vibrio cholerae*. Nat. Rev. Microbiol. **3:**611–620.
10. **Butler, S. M., E. J. Nelson, N. Chowdhury, S. M. Faruque, S. B. Calderwood, and A. Camilli.** 2006. Cholera stool bacteria repress chemotaxis to increase infectivity. Mol. Microbiol. **60:**417–426.
11. **Camilli, A., and J. J. Mekalanos.** 1995. Use of recombinase gene fusions to identify *Vibrio cholerae* genes induced during infection. Mol. Microbiol. **18:**671–683.
12. **Constantin de Magny, G., R. Murtugudde, M. R. Sapiano, A. Nizam, C. W. Brown, A. J. Busalacchi, M. Yunus, G. B. Nair, A. I. Gil, C. F. Lanata, J. Calkins, B. Manna, K. Rajendran, M. K. Bhattacharya, A. Huq, R. B. Sack, and R. R. Colwell.** 2008. Environmental signatures associated with cholera epidemics. Proc. Natl. Acad. Sci. USA **105:**17676–17681.
13. **Correa, N. E., J. R. Barker, and K. E. Klose.** 2004. The *Vibrio cholerae* FlgM homologue is an anti-σ^{28} factor that is secreted through the sheathed polar flagellum. J. Bacteriol. **186:**4613–4619.
14. **Correa, N. E., C. M. Lauriano, R. McGee, and K. E. Klose.** 2000. Phosphorylation of the flagellar regulatory protein FlrC is necessary for *Vibrio cholerae* motility and enhanced colonization. Mol. Microbiol. **35:**743–755.
15. **Correa, N. E., F. Peng, and K. E. Klose.** 2005. Roles of the regulatory proteins FlhF and FlhG in the *Vibrio cholerae* flagellar transcription hierarchy. J. Bacteriol. **187:**6324–6332.

16. **Cserzo, M., E. Wallin, I. Simon, G. von Heijne, and A. Elofsson.** 1997. Prediction of transmembrane alpha-helices in prokaryotic membrane proteins: the dense alignment surface method. Protein Eng. **10:**673–676.
17. **Donnenberg, M. S., and J. B. Kaper.** 1991. Construction of an *eae* deletion mutant of enteropathogenic *Escherichia coli* by using a positive-selection suicide vector. Infect. Immun. **59:**4310–4317.
18. **Freter, R., and G. W. Jones.** 1976. Adhesive properties of *Vibrio cholerae*: nature of the interaction with intact mucosal surfaces. Infect. Immun. **14:**246–256.
19. **Freter, R., P. C. M. O'Brien, and M. S. Macsai.** 1981. Role of chemotaxis in the association of motile bacteria with intestinal mucosa: in vivo studies. Infect. Immun. **34:**234–240.
20. **Freter, R., and P. C. M. O'Brien.** 1981. Role of chemotaxis in the association of motile bacteria with intestinal mucosa: chemotactic responses of *Vibrio cholerae* and description of motile nonchemotactic mutants. Infect. Immun. **34:**215–221.
21. **Goymer, P., S. G. Kahn, J. G. Malone, S. M. Gehrig, A. J. Spiers, and P. B. Rainey.** 2006. Adaptive divergence in experimental populations of *Pseudomonas fluorescens*. II. Role of the GGDEF regulator WspR in evolution and development of the wrinkly spreader phenotype. Genetics **173:**515–526.
22. **Guzman, L.-M., D. Beblin, M. J. Carson, and J. Beckwith.** 1995. Tight regulation, modulation, and high-level expression by vectors containing the arabinose P_{BAD} promoter. J. Bacteriol. **177:**4121–4130.
23. **Hanahan, D.** 1983. Studies on transformation of *Escherichia coli* with plasmids. J. Mol. Biol. **166:**557–580.
24. **Hartley, D. M., J. G. Morris, Jr., and D. L. Smith.** 2006. Hyperinfectivity: a critical element in the ability of *V. cholerae* to cause epidemics? PLoS Med. **3:**e7.
25. **Hirokawa, T., S. Boon-Chieng, and S. Mitaku.** 1998. SOSUI: classification and secondary structure prediction system for membrane proteins. Bioinformatics **14:**378–379.
26. **Hoch, J. A., and T. J. Silhavy.** 1995 Two-component signal transduction. ASM Press, Washington, DC.
27. **Horton, R. M., H. D. Hunt, S. N. Ho, J. K. Pullen, and L. R. Pease.** 1989. Engineering hybrid genes without the use of restriction enzymes: gene splicing by overlap extension. Gene **77:**61–68.
28. **Huq, A., E. B. Small, P. A. West, M. I. Huq, R. Rahman, and R. R. Colwell.** 1983. Ecological relationships between *Vibrio cholerae* and planktonic crustacean copepods. Appl. Environ. Microbiol. **45:**275–283.
29. **Kanehisa, M., M. Araki, S. Goto, M. Hattori, M. Hirakawa, M. Itoh, T. Katayama, S. Kawashima, S. Okuda, T. Tokimatsu, and Y. Yamanishi.** 2008. KEGG for linking genomes to life and the environment. Nucleic Acids Res. **36:**D480–D484.
30. **Kanehisa, M., and S. Goto.** 2000. KEGG: Kyoto encyclopedia of genes and genomes. Nucleic Acids Res. **28:**27–30.
31. **Kanehisa, M., S. Goto, M. Hattori, K. F. Aoki-Kinoshita, M. Itoh, S. Kawashima, T. Katayama, M. Araki, and M. Hirakawa.** 2006. From genomics to chemical genomics: new developments in KEGG. Nucleic Acids Res. **34:**D354–D357.
32. **Klose, K. E., and J. J. Mekalanos.** 1998. Differential regulation of multiple flagellins in *Vibrio cholerae*. J. Bacteriol. **180:**303–316.
33. **Klose, K. E., and J. J. Mekalanos.** 1998. Distinct roles of an alternative sigma factor during both free-swimming and colonizing phases of the *Vibrio cholerae* pathogenic cycle. Mol. Microbiol. **28:**501–520.
34. **Koch, R.** 1884. An address on cholera and its bacillus. Br. Med. J. **2:**403–407.
35. **Kolter, R., M. Inuzuka, and D. R. Helinski.** 1978. Trans-complementation-dependent replication of a low molecular weight origin fragment from plasmid R6K. Cell **15:**1199–1208.
36. **Lauriano, C. M., C. Ghosh, N. E. Correa, and K. E. Klose.** 2004. The sodium-driven flagellar motor controls exopolysaccharide expression in *Vibrio cholerae*. J. Bacteriol. **186:**4864–4874.
37. **Lee, S. H., S. M. Butler, and A. Camilli.** 2001. Selection for in vivo regulators of bacterial virulence. Proc. Natl. Acad. Sci. USA **98:**6889–6894.
38. **Liu, Z., T. Miyashiro, A. Tsou, A. Hsiao, M. Goulian, and J. Zhu.** 2008. Mucosal penetration primes *Vibrio cholerae* for host colonization by repressing quorum sensing. Proc. Natl. Acad. Sci. USA **105:**9769–9774.
39. **Manoil, C.** 1991. Analysis of membrane protein topology using alkaline phosphatase and beta-galactosidase gene fusions. Methods Cell Biol. **34:**61–75.
40. **Martin, P. R., A. A. Watson, T. F. McCaul, and J. S. Mattick.** 1995. Characterization of a five-gene cluster required for the biogenesis of type 4 fimbriae in *Pseudomonas aeruginosa*. Mol. Microbiol. **16:**497–508.
41. **McCarter, L. L.** 2001. Polar flagellar motility of the *Vibrionaceae*. Microbiol. Mol. Biol. Rev. **65:**445–462.
42. **Meibom, K. L., M. Blokesch, N. A. Dolganov, C. Y. Wu, and G. K. Schoolnik.** 2005. Chitin induces natural competence in *Vibrio cholerae*. Science **310:**1824–1827.
43. **Meibom, K. L., X. B. Li, A. T. Nielsen, C. Y. Wu, S. Roseman, and G. K. Schoolnik.** 2004. The *Vibrio cholerae* chitin utilization program. Proc. Natl. Acad. Sci. USA **101:**2524–2529.
44. **Merrell, D. S., S. M. Butler, F. Qadri, N. A. Dolganov, A. Alam, M. B. Cohen, S. B. Calderwood, G. K. Schoolnik, and A. Camilli.** 2002. Host-induced epidemic spread of the cholera bacterium. Nature **417:**642–645.
45. **Miller, V. L., and J. J. Mekalanos.** 1988. A novel suicide vector and its use in construction of insertion mutations: osmoregulation of outer membrane proteins and virulence determinants in *Vibrio cholerae* requires *toxR*. J. Bacteriol. **170:**2575–2583.
46. **Morales, V. M., A. Backman, and M. Bagdasarian.** 1991. A series of wide-host-range low-copy-number vectors that allow direct screening for recombinants. Gene **97:**39–47.
47. **Morris, D. C., F. Peng, J. R. Barker, and K. E. Klose.** 2008. Lipidation of an FlrC-dependent protein is required for enhanced intestinal colonization by *Vibrio cholerae*. J. Bacteriol. **190:**231–239.
48. **Nalin, D. R.** 1976. Cholera, copepods, and chitinase. Lancet **7992:**958.
49. **Nielsen, A. T., N. A. Dolganov, G. Otto, M. C. Miller, C. Y. Wu, and G. K. Schoolnik.** 2006. RpoS controls the *Vibrio cholerae* mucosal escape response. PLoS Pathog. **2:**e109.
50. **Prouty, M. G., N. E. Correa, and K. E. Klose.** 2001. The novel sigma54- and sigma28-dependent flagellar gene transcription hierarchy of *Vibrio cholerae*. Mol. Microbiol. **39:**1595–1609.
51. **Provenzano, D., and K. E. Klose.** 2000. Altered Expression of the ToxR-regulated porins OmpU and OmpT diminishes *Vibrio cholerae* bile resistance, virulence factor expression, and intestinal colonization. Proc. Natl. Acad. Sci. USA **97:**10220–10224.
52. **Pruzzo, C., L. Vezzulli, and R. R. Colwell.** 2008. Global impact of *Vibrio cholerae* interactions with chitin. Environ. Microbiol. **10:**1400–1410.
53. **Quinones, M., H. H. Kimsey, and M. K. Waldor.** 2005. LexA cleavage is required for CTX prophage induction. Mol. Cell **17:**291–300.
54. **Rawlings, T. K., G. M. Ruiz, and R. R. Colwell.** 2007. Association of *Vibrio cholerae* O1 El Tor and O139 Bengal with the copepods *Acartia tonsa* and *Eurytemora affinis*. Appl. Environ. Microbiol. **73:**7926–7933.
55. **Reidl, J., and K. E. Klose.** 2002. *Vibrio cholerae* and cholera: out of the water and into the host. FEMS Microbiol. Rev. **26:**125–139.
56. **Roberts, A., G. D. Pearson, and J. J. Mekalanos.** 1992. Cholera vaccines strains derived from a 1991 Peruvian isolate of *Vibrio cholerae* and other El Tor strains, p. 43–47. Proc. 28th Joint Conf. U.S.-Jpn. Coop. Med.-Sci. Program Cholera Relat. Diarrhea. Dis.
57. **Schild, S., A. K. Lamprecht, and J. Reidl.** 2005. Molecular and functional characterization of O antigen transfer in *Vibrio cholerae*. J. Biol. Chem. **280:**25936–25947.
58. **Schild, S., E. J. Nelson, A. L. Bishop, and A. Camilli.** 2009. Characterization of *Vibrio cholerae* outer membrane vesicles as a candidate vaccine for cholera. Infect. Immun. **77:**472–484.
59. **Schild, S., E. J. Nelson, and A. Camilli.** 2008. Immunization with *Vibrio cholerae* outer membrane vesicles induces protective immunity in mice. Infect. Immun. **76:**4554–4563.
60. **Schild, S., R. Tamayo, E. J. Nelson, F. Qadri, S. B. Calderwood, and A. Camilli.** 2007. Genes induced late in infection increase fitness of *Vibrio cholerae* after release into the environment. Cell Host Microbe **2:**264–277.
61. **Simons, R. W., F. Houman, and N. Kleckner.** 1987. Improved single and multicopy lac-based cloning vectors for protein and operon fusions. Gene **53:**85–96.
62. **Sonnhammer, E. L., G. von Heijne, and A. Krogh.** 1998. A hidden Markov model for predicting transmembrane helices in protein sequences. Proc. Int. Conf. Intell. Syst. Mol. Biol. **6:**175–182.
63. **Tusnady, G. E., and I. Simon.** 1998. Principles governing amino acid composition of integral membrane proteins: application to topology prediction. J. Mol. Biol. **283:**489–506.
64. **Watnick, P., and R. Kolter.** 1999. Steps in the development of a *Vibrio cholerae* El Tor biofilm. Mol. Microbiol. **34:**586–595.